Development of an engineering optimization tool for miniature Pulsed Plasma Thrusters

IEPC-2015-51

Presented at Joint Conference of 30th International Symposium on Space Technology and Science 34th International Electric Propulsion Conference and 6th Nano-satellite Symposium, Hyogo-Kobe, Japan July 4 – 10, 2015

Igor O. Golosnoy [1] and Stephen B. Gabriel [2]
University of Southampton, FPSE, ECS, Highfield, Southampton, SO17 1BJ, UK

Simone Ciaralli [3] and Michele Coletti [4]
Mars Space Ltd, Unit 61, Basepoint Business Center, Southampton, SO14 5FE, UK

Abstract: Pulsed Plasma Thrusters (PPT) are an established technology for compact thrust propulsion systems. Although PPT optimization has been performed previously it requires complex numerical codes. A 0D pulsed inductive acceleration model has been developed which links together the dynamics of the current sheet with the plasma dimensions and ionization processes. The model novelty is in a self-consistent estimation of the plasma sheet properties (temperature, density, thickness) driven by the magnetic pinch pressure and propellant ablation together with its simplicity. Parametric studies have been performed in an attempt to arrive at optimized design solutions for small PPTs.

Nomenclature

a	=	energy accommodation coefficient
C	=	capacitance
e	=	electron charge
h	=	distance between electrodes
H	=	enthalpy
I	=	electric current
J	=	ionization potential
k_B	=	Boltzmann constant
L	=	inductance
m	=	mass
M	=	molar mass
n	=	concentration
P	=	pressure
Q	=	power
q	=	energy flux
R	=	resistance
T	=	temperature
t	=	time
v,u	=	velocity

[1] Associate Professor, Faculty of Physical Sciences and Engineering, i.golosnoy@soton.ac.uk
[2] Professor, Faculty of Physical Sciences and Engineering, sbg2@soton.ac.uk
[3] Electric Propulsion Engineer, simone.ciaralli@mars-space.co.uk
[4] Director, michele.coletti@mars-space.co.uk

Z = charge
V = electric potential
w = width of chamber (distance between propellant bars)
z = coordinate along direction of exhaust
δ = thickness of current sheet
φ = material work function
χ = ionization frequency
Λ = Coulomb logarithm
μ = mass ratio
ρ = density
σ = electric conductivity

Indexes
0 = neutrals
e = electrons
i = ions
h = heavy particles (ions, neutrals)
av = average
t = time

I. Introduction

It is generally accepted that the discharge evolution of a PPT can be described to a first approximation by a circuit model where the plasma sheet is represented by the discrete and time-constant elements of an RLC series circuit. The circuit model is then coupled with the conservation of the plasma momentum that depends on the discharge current and the inductance change per unit length. This system of equations is called the "snowplough model" [1]. The classic approach in solving it is to assume that all the inputs parameters are constant hence relying on the availability of the experimental data needed to determine the plasma characteristics and the ablated mass. Most of the optimization efforts carried out so far were strongly based on experimental measurements[2-8]. Given the complexity of these processes (coupling of thermal, chemical electromagnetic and gas and plasma dynamics processes), we propose the development of a model where a PPT is represented as an RLC circuit but with electrical parameters that are variable in time and space and obtained from the numerical simulation of the different physical processes hence removing the need of extensive test campaigns. The model will have to include: the estimation of the magnetic field generated by the discharge current, the characterization of the plasma column in the discharge (in terms of its size, ionization level, electrons and heavy particle temperature and resistivity) and the quantification of the propellant ablation as a function of the discharge parameters. Assuming a given thruster geometry, we propose an innovative model that will calculate the space and time variable parameters to use as inputs for the standard PPT snowplough model. The snowplough model will then allow for the calculation of the PPT performances in terms of impulse bit, specific impulse and total impulse. By iteratively changing the thruster geometry and input parameters the model can be used to determine the best configuration, intended as the one delivering the highest Isp and total impulse, can be selected.

The magnetic field can be calculated in 3D from first principle once the thruster geometry is known. The propellant ablation model can be derived starting from past modeling efforts[8,9] or based on semi-empiric relations derived from the analysis of the data available in the literature[10]. A plasma model has developed using simplifying assumptions justified by past experimental observations and supported by the model predictions. This model is based on 3 simplifying assumptions, quasineutrality, full dissociation of PTFE into F and C and that the plasma is in a state of Local Thermodynamic Equilibrium (LTE). A 0D model is developed for plasma motion, solving the conservation of momentum equations and time marching. It is known that substantial amount of ablated material is not ionized due to short dwelling times. The novel model takes into account both plasma and gas components of the impulse bit.

The primary motivation for this work was to develop a simple, but more accurate than the classical models available which rely heavily on empirical data, which was quick to run and would avoid time-consuming, iterative and expensive testing to optimize the design or at least to arrive at a thruster with performance that meets a set of mission requirements. Sophisticated and comprehensive numerical models like that in Ref.9 are not generally

available so something else was needed and in a limited time since the total time period for the funded work was extremely short at 12 months.

The paper is divided into 3 parts. The first describes the model itself while the second is devoted to a comparison of the model results with experimental data from the micro-PPTs developed by Mars Space Ltd. in collaboration with the University of Southampton, with the last part presenting some conclusions and brief comments on future work.

II. The Model Framework

The overall device model includes sub-models coupled together. We consider

- Electric circuit (coupled with the plasma and motion of the current sheet)
- Plasma properties (coupled to the circuit, ablation, ionization and current sheet)
- Current sheet geometry and motion (coupled to the circuit and plasma properties)
- Ablation (coupled to the plasma and current sheet)

A. Geometry

The schematic of the chamber geometry is given in Fig.1. The chamber forms a nozzle so the gas-dynamic contribution of the thrust can be increased. Also the electrodes are extended beyond the side Teflon blocks to utilize remaining charge on the capacitor for further acceleration of the plasma sheet. The plasma sheet is assumed to be a rectangular with length $h(z)$, width $w(z)$ and thickness $\delta(z,t)$ which varies as plasma mass increases due to ablation of Teflon blocks. Both h and w are fixed by the chamber walls but $\delta(z,t)$ varies to accommodate an ablated mass in the plasma sheet volume, keeping in mind that the plasma density is a function of plasma temperature T, pressure P and composition (electrons concentration n_e, ions concentration n_i, average ionization $Z_{av}=n_e/n_i$ and concentration of neutrals n_0).

$$\delta(z,t)=\frac{m_p(t)}{\rho(t)h(z)w(z)}\tilde{} \tag{1}$$

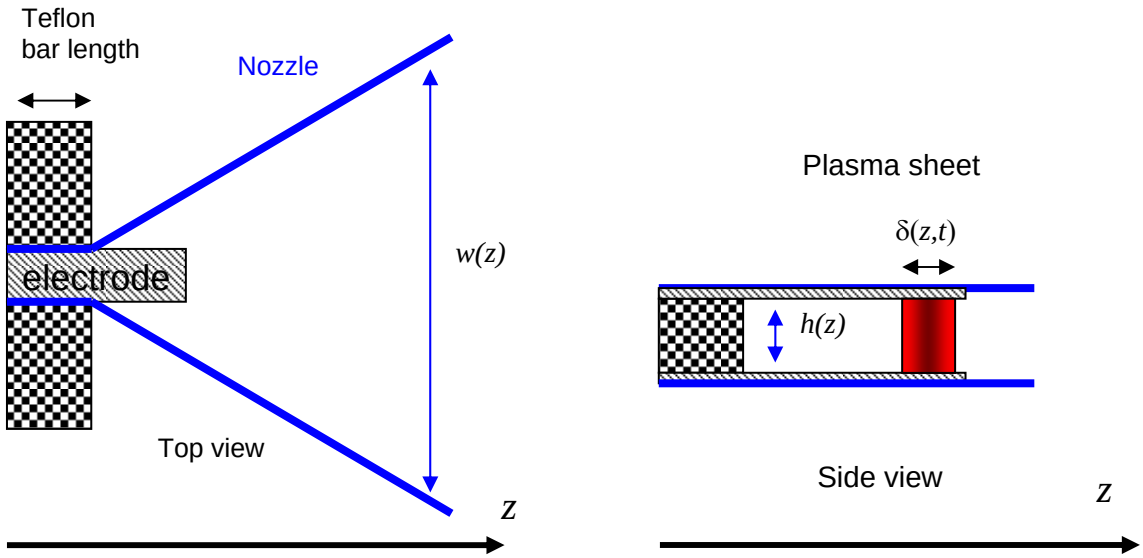

Figure 1. Model Geometry of PPT chamber.

For the plasma an ideal gas law is assumed and contribution of electrons to the mass density is ignored with approximate relation is

$$P \approx \left(1+\frac{n_e}{n_i+n_0}\right)\rho\frac{R_g T}{M_{av}},.. \rho \approx m_h(n_i+n_0). \tag{2}$$

where P is plasma pressure, ρ is plasma density, R_g is the universal gas constant, T plasma temperature, M_{av}=16.7 10^{-3} kg/mol is an average molar mass of 33% C – 67% F mixture, m_h=16.7 a.u. is an average mass of heavy particle in this mixture.

Classic snowplough model for plasma sheet position *z(t)* is written in the momentum form:

$$\frac{d}{dt}\left(m_p v_p\right)=\frac{1}{2}\frac{dL}{dz}I^2,\ \frac{dz}{dt}=v_p \tag{3}$$

B. Electric circuit

The discharge is modeled by a simplified LCR circuit:

$$L\frac{dI}{dt}+RI(t)+V(t)=0,\ I=-C\frac{dV}{dt} \tag{4}$$

with total inductance $L=L_d(z)+L_p$, device inductance $L_d(z)$ depends on position of current sheet z with $L_d(z=0)$=18nH, plasma self-inductance is ignored $L_p \approx 0$, resistance is mainly due to plasma with small contribution from electrodes and capacitors bank $R=R_d+R_p$, measured $R_d=5m\Omega$, and resistance of plasma is driven both by plasma conductivity σ and geometry:

$$R_p=\frac{1}{\sigma_p}\frac{h_{eff}}{w_{eff}\delta(z,t)} \tag{5}$$

$$\frac{h_{eff}}{w_{eff}}=\frac{h(z)-w(z)+w_{el}}{w(z)}+\frac{w(z)-w_{el}}{w_{el}} \tag{6}$$

Eq.(6) takes into account funneling of plasma sheet current towards of the electrodes when the channel is wider than electrodes. For the case simple case $w(z)=w_{el}$ it reduces to a standard formula for resistance of a conducting sheet. In (5) the main contribution comes from *e-i* collisions[11,12] and for a multi-charged plasma it can be approximated by

$$\sigma_p=0.4135\frac{\left(4\pi\varepsilon_0\right)^2\left(k_B T\right)^{3/2}}{Z_{av}e^2 m_e^{1/2}\ln\Lambda}. \tag{7}$$

where ε_0 is vacuum permittivity, k_B is Boltzman constant, m_e mass of electron, T and Z_{av} is plasma temperature and average ionization respectively, lnΛ is the Coulomb logarithm. The circuit model is coupled with plasma model via conductivity (7) and with geometry via (1).

The current flowing through the plasma sheet creates an average pinch pressure

$$P_p=\frac{\mu_0 I^2}{4w} \tag{8}$$

C. Plasma properties

In this study plasma Equation of State and kinetic coefficients are taken for LTE conditions. Model estimates for energy transfer time between electrons and ions show that something between 1ns-50ns would be required for the plasma temperatures predicted (maximum relaxation time correspond to the highest predicted temperature 15 eV which drops to 3-5eV at the exhaust plane (end of the nozzle) , see Section IV). In the experiments since the rise to the maximum temperature value 15 eV takes 500ns to achieve and the electron density is above 10^{23} m^{-3}, it is believed that plasma will be in LTE, at least approximately. The temperature is assumed to be uniform in the sheet up to the surfaces, $T_i = T_e = T$. This assumption neglects changes in plasma temperature next to the evaporated surface. The plasma composition $n_e(P,T), n_i(P,T), n_0(P,T)$ can be calculated via Saha equation[11,13] as well as its conductivity eq.(7) and specify enthalpy *H(P,T)*. Although the pressure does vary as the sheet moves in the chamber, it is assumed that on average the pressure is equal to time averaged pinch pressure (8) during the first discharge cycle $<P_p(t)>$.

Joule power input in the plasma $I^2 R_p$ results in its heating but a substantial amount of energy is lost to the surfaces and escapes in the form of radiation. Energy flux to the dielectric (Teflon) surface is given in section 2.4, with the radiation being calculated according to Bremsstrahlung only[11,13]:

$$q_{rad} = 1.57 \cdot 10^{-40} Z_{av}^2 n_e n_i T^{1/2} \tag{9}$$

and overall losses are $Q_{rad} = q_{rad}(wh\delta)$. Losses at the dielectric surface Q_{diel} are given in section 2.4. The processes at the electrodes are complex[11,13] and their detailed consideration would make the model too complicated. Based on the fact that the predicted plasma temperature reaches ~10eV and above, the main heat flux from the plasma will be generated by bombardment of charged particles on electrodes, i.e.

$$Q_{elec} = 2 \cdot \left| \frac{I}{e} \right| \frac{5k_B T}{2} + \left[|I_i| (V_c + J_{av} - \varphi_{Cu}) - |I_e| \varphi_{Cu} \right] + |I| \left[V_a + \varphi_{Cu} \right] \tag{10}$$

where $\frac{I_e}{I}$~0.8, $\frac{I_i}{I}$~0.2 are typical fractions of electron and ion cathode currents, V_a=5V, V_c=5V, φ_{Cu}=4.5V are anodic, cathodic potential falls, work function for copper[11]. Since constant pressure is assumed, the energy balance for mass of the sheet m_p is written in an enthalpy form with H being an enthalpy per unit mass:

$$\frac{d}{dt}\left(m_p H \right) = I^2 R_p - Q_{rad} - Q_{diel} - Q_{elec} \tag{11}$$

D. Teflon ablation

The model is based on Ref.8 with additional simplifications as discussed below. Particles fluxes to PTFE surfaces from plasma can be expressed as

$$\varphi_e = \frac{1}{4} n_e \left(\frac{8k_B T}{\pi m_h} \right)^{1/2}, \varphi_i = \frac{\varphi_e}{Z_{av}}, \varphi_0 = \frac{1}{4} n_0 \left(\frac{8k_B T}{\pi m_h} \right)^{1/2} \tag{12}$$

Electrons slow down due to the sheath with potential

$$\phi = \left(\frac{k_B T}{2e} \right) \ln \left(\frac{m_h}{m_e} \right) \tag{13}$$

They lose energy on impact with the surface and deposit at the top layer.

$$q_e = \varphi_e a_e 2k_B\left(T - T_s\right), q_i = \varphi_i a_i\left[2k_B\left(T - T_s\right) + Z_{av} e\phi\right], q_0 = \varphi_0 a_0 2k_B\left(T - T_s\right) \tag{14}$$

Energy accommodation coefficients of electrons, ions and neutrals a_e, a_i, a_0 can be expressed in terms of the mass ratio of incoming particle and an average mass of atom in PTFE:

$$a_x = \frac{2\mu_x}{\left(1+\mu_x\right)^2}, \mu_x = \frac{m_x}{m_h} \tag{15}$$

Effectively, for heavy particle a=0.5 and it can be neglect for electrons. The ablation flux is driven by Langmuir's relation[14]:

$$\Gamma = \left(\frac{m_h}{2\pi k_B T}\right)^{1/2} P_{vap}. \tag{16}$$

The vaporization pressure of PTFE is

$$P_{vap} = P_c \exp\left(-\frac{T_c}{T_s}\right) \tag{17}$$

where $P_c = 1.84\times10^{15}$ Pa , $T_c = 20815$ K and T_s is PTFE surface temperature.

On the surface the energy input from particles impacts and radiation is balanced by energy losses to evaporation (low thermal diffusivity of PTFE and short exposure times allows to neglect heating of PTFE bulk):

$$q_i + q_e + q_0 + q_{rad} = q_{abl}. \tag{18}$$

$$q_{abl} = \Gamma\left(\frac{2k_B T}{m_h} + H_{pol} + H_{ev}\right). \tag{19}$$

where H_{pol} = 1.58 MJ/kg, and H_{ev} = 25 MJ/kg are polymerization and evaporation enthalpies of PTFE[15,16,17]. Value of H_{ev} has been increased by a factor of 2 in comparison with Ref.15 but consistent with Ref.16,17 and incorporates dissociation effects since only an atomic (no molecules) gas-plasma mixture is considered in Saha model.

Equations (12)-(19) are solved with known plasma properties to find the self-consistent propellant surface temperature T_s.

E. Ionization of ablated material

Under intensive evaporation neutral atoms enter the plasma near the surface region where electron ionization capabilities are reduced due to slowdown in the sheath. To find the ionization frequency a standard classical formula[13] is utilized (average ionization threshold J_{av}=15.7eV and Maxwell velocity distribution of electrons have been assumed):

$$\chi_{ion} = \frac{\pi e^4}{\left(4\pi\varepsilon_0\right)^2 J_{av}^2} u_e n_e \exp\left(-\frac{J_{av}}{k_B T}\right). \tag{20}$$

with the average velocity of electrons corrected for the deceleration in the pre-sheath:

$$u_e = \left(\frac{8k_B T}{\pi m_e}\right)^{1/2}\left(\frac{m_e}{m_h}\right)^{1/2} \sim \tag{21}$$

The fraction of ionized atoms increases with time according to

$$n_{ion}(t)/n_{at}(t=0) = \left(1-\exp(-\chi_{ion}t)\right) \tag{22}$$

but the atoms entering the sheet at different points stay within the hot region for different times. Integration over the dwelling time up to the max $\Delta t_{\max} = z/v_p$ results in the mass entering the sheet being given by:

$$\frac{dm_p}{dt} = \frac{dm_{abl}}{dt}\left(1-\frac{v_p}{\chi_{ion}\delta}\exp\left(-\frac{\chi_{ion}\delta}{v_p}\right)\right) \tag{23}$$

$$\frac{dm_{abl}}{dt} = \delta w\Gamma_{..}, \quad \frac{dm_{gas}}{dt} = \frac{d\left(m_{abl}-m_p\right)}{dt}. \tag{24}$$

where m_{abl} is the overall ablated mass, and m_p is the addition to the plasma sheet. In (23)-(24) the presence of neutrals within the plasma sheet is ignored since the temperature exceeds 10000 K.

F. Solution method

The model has been implemented in COMSOL commercial software and solved using a fully coupled solver. The time step was taken to be 1ns to capture fast changes in plasma properties. To check for convergence, the time step was reduced to 0.5ns and 0.1ns and it resulted in less than 5% variations in the model outputs.

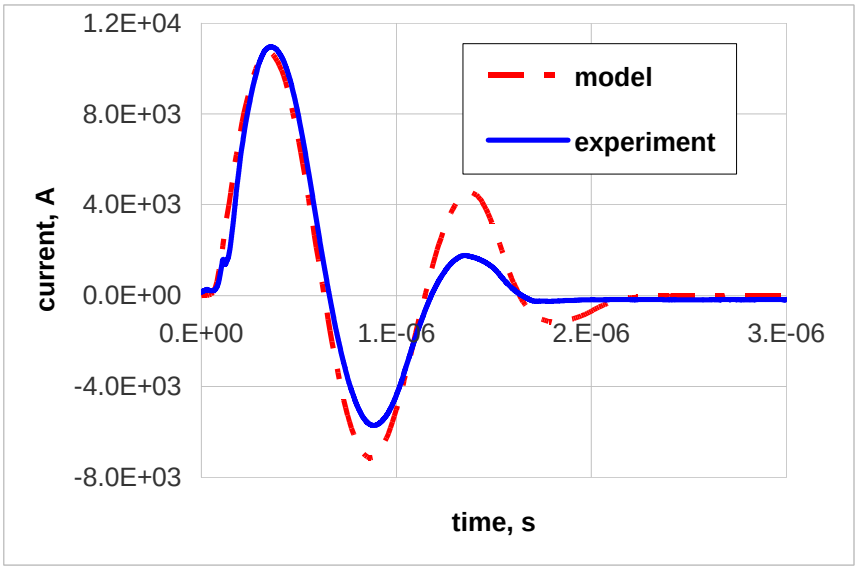

Figure 2. Comparison of predicted and measured current for PPT chamber given in Fig.1.

III. Model Verification

The model predictions have been compared with experimental measurements done on the setup with dimensions specified on Figure 1. The capacitor stored energy was 2 J. It is assumed that after the initial spark at 8200K ablated

a mass of 10^{-2} μg (the model is insensitive to these inputs). The comparison is given in the first two columns of Table 1. Overall, the model agrees with the measured integral quantities within the experimental errors. Of course such oversimplified model based on global energy balance cannot capture all details of plasma-gas expansion and it can be seen from Figure 2. The discrepancy between measured and predicted current at later stages of the expansion is due to neglecting of plasma cooling during an expansion at the nozzle. Currents are relatively low at this stage and such an assumption does not affect the final impulse.

Teflon bar length (mm)	***experiment (5mm)***	***5***	***7***	***9***
Total ablated mass, μg	**6.5 +/-2%**	**6.5**	**10.6**	**15**
Mass of current sheet (ionised), μg		2.8	4	4.9
Maximum plasma temperature, eV		**15**	**15**	**15**
Plasma temperature at exhaust, eV		**4.3**	**3.5**	**3**
Teflon surface temperature, K		920	920	920
Ablation duration, μs		0.8	1.1	1.5
Total Impulse bit, μN·s	**39.2 +/- 3.5**	**38.5**	**51**	**64.5**
Electromagnetic part of impulse, μN·s		24.5	25.5	25.5
Thermal part of impulse, μN·s		14	25.5	39
Specific impulse total, s	**615**	**610**	**490**	**440**

Table 1. Predicted dependence of PPT performance as a function of Teflon bars length and comparison with experiment. Height of the chamber (distance between electrodes) is 10mm, energy in the capacitor bank is 2 J. Other dimensions as in Fig.1.

IV. Parametric studies

To find an optimum configuration of the PPT thruster, a set of design parameters has been varied. 2 parameters were concentrtated on: the height of the discharge chamber (distance between electrodes), Table 2, and the width of the Teflon bars, Table 1.

An increase in the height of the chamber results in a larger surface area of Teflon exposed to the plasma which in turn would give a higher mass bit but reduces the current (via reduced plasma temperature and conductivity) and electromagnetic acceleration, Figure 3. A smaller height reduces the ablation mass, results in higher acceleration and shorter ablation duration, Figure 4.

Chamber height, h (mm)	***8***	***10***	***12***	***14***
Total ablated mass, μg	**3.0**	**6.5**	**11.5**	**17.6**
Mass of current sheet (ionised), μg	1.2	2.8	4.8	6.5
Maximum plasma temperature, eV	**15.5**	**15**	**14**	**13.5**
Plasma temperature at exhaust, eV	**6.4**	**4.3**	**3**	**2.5**
Teflon surface temperature, K	930	920	910	890
Ablation duration, μs	0.4	0.8	1.1	1.5
Total Impulse bit, μN·s	**30.7**	**38.5**	**48**	**61**
Electromagnetic part of impulse, μN·s	24	24.5	22	18
Thermal part of impulse, μN·s	6.7	14	26	43
Specific impulse total, s	**1050**	**610**	**420**	**350**

Table 2. Predicted dependence of PPT performance as a function of the distance between electrodes). Teflon bars length is 5mm, energy in the capacitor bank is 2 J. Other dimensions as in Fig.1.

Shorter electrode separations initially result in higher current (due to low resistance), Fig.3, and actually larger mass to be ablated in the first 0.2-0.3 μs after the initiation, Fig.4. But since the temperature of plasma builds up, its conductivity increases slowly at temperatures above 3 eV and larger distances on average produce very similar ablation rates, see Fig.4 at 0.5 μs. It is due to the larger surface of propellant bars exposed to the hot plasma. In the case of 8 mm chamber the sheet accelerates strongly but after that slows down due to large ablated mass enters the sheet until it reaches the end of the bars (5mm) in 0.4 μs. At this point a significant charge is left on the capacitor

bank. As the sheet continues to propagate along the electrodes (up to 15mm) it heats up by additional 3eV, accelerates further and may reach a very high velocity of 19 km/s, Figure 5. Similar effects can be seen for 10 mm distance, but in this case it takes 0.75 μs to reach the bars end. A smaller charge is left on the capacitor bank and the additional temperature rise is only 1eV. Nevertheless it still provides a noticeable increase in the sheet velocity. Increasing the distance further to 12mm and 14mm results in almost complete discharges while the current sheet is in the contact with the Teflon bars. The plasma temperature reduces slowly as well as the exhaust velocity.

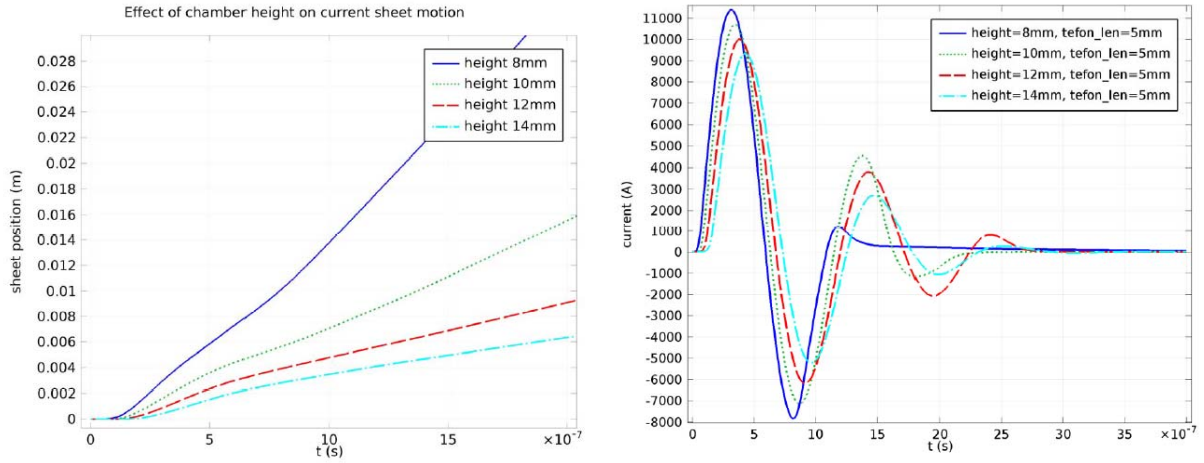

Figure 3. Predicted effect of the distance between electrodes on motion of the current sheet and the current. (a) sheet position (compare with Teflon bars length 0.005m); (b) current waveform

The electromagnetic part of the impulse is only weakly affected by changer in the electrode separation, see Table 2, since the current waveform varies only slightly, Fig.3b. Opposite to that the thermodynamic part of the impulse rises significantly with the ablated mass and the large distance (height) promotes the noticeable increase, Table 2. But this increase in total impulse is due to a significant increase in the mass loss per shot, so the specific impulse drops significantly. So optimal configuration corresponds to a minimal possible chamber height which delivers the required impulse bit. In this case we can achieve a maximum specific impulse and a minimum mass of the propellant bars.

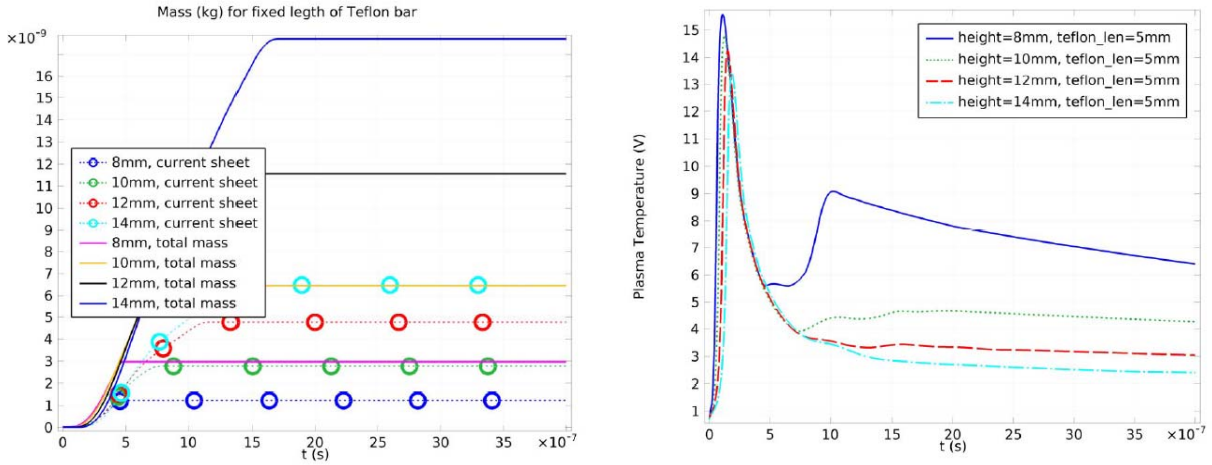

Figure 4. Predicted effect of the distance between electrodes on (a) total ablated mass and ionized fraction; (b) plasma temperature in eV.

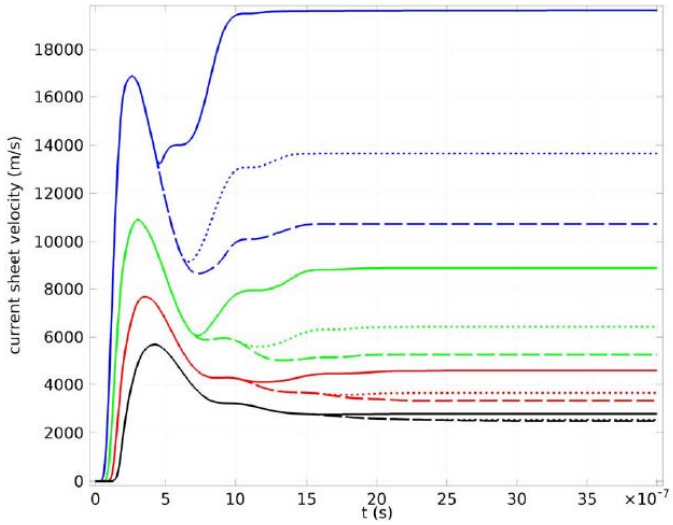

Figure 5. Predicted velocity of the current sheet: color code for distance between electrodes (blue – 8mm, green – 10mm, red – 12mm, black – 14mm), line style for different length of Teflon bars: solid – 5mm, dotted – 7mm, dashed – 9mm.

An increase in the thermodynamic part of the impulse can be achieved by increasing the propellant bar width not height. In this case the initial current waveform is unaffected, see Fig.6a, and the electromagnetic part of the impulse is the same, see Table 1. Wider bars increase the ablated mass and contribute to thermodynamic part of the impulse. It still reduces specific impulse but to a lesser extent. Such an approach may be preferable in comparison with an increase in the chamber height, since the latter reduces the electromagnetic component of the impulse bit.

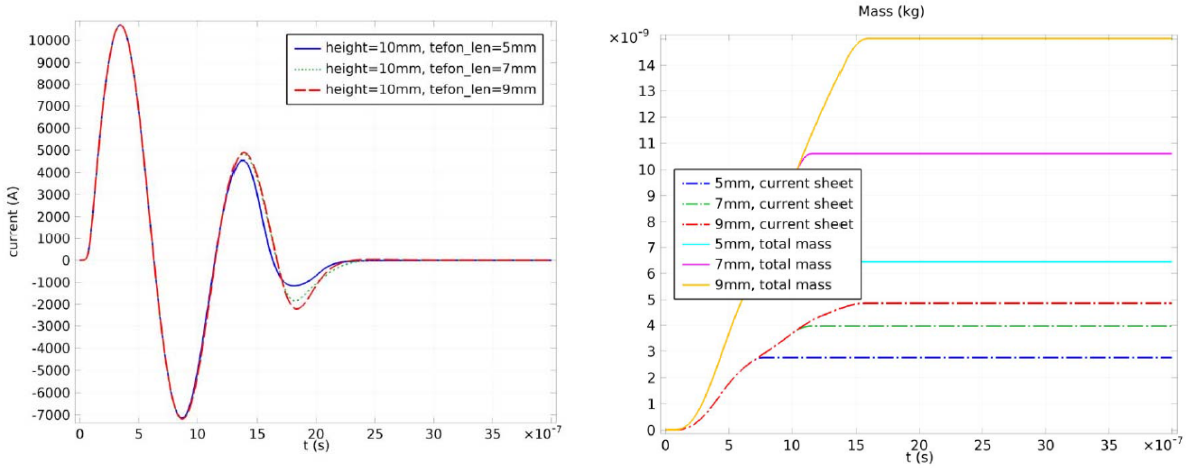

Figure 6. Predicted effect of the propellant bars length (a) current waveforms; (b) total ablated mass and ionized fraction.

V. Conclusion

It was shown that a simple 0D pulsed inductive acceleration model can be successfully used to optimize PPT design. A key feature of the model is a self-consistent consideration of the plasma properties and the ablation process. It was shown that a required impulse bit can be achieved by varying the cross-section geometries of the propellant bars while keeping their cross-sectional areas (and their masses) constant. An impulse bit of 50 μN·s per

2 J shot can be achieved with a specific impulse of 500 s. The future work will include extended parametric studies, assembly and testing of several PPTs with most promising configurations, which will aid in validation of the model.

Acknowledgments

This work has been supported by EPSRC via grant EP/M506783/1 and by TSB via grant 101884.

References

[1] Jahn R., *Physics of Electric Propulsion*, McGraw-Hill, New York, 1968.

[2] Palumbo D.J. and Guman W.J., "Effects of Propellant and Electrode Geometry on Pulsed Ablative Plasma Thruster Performance", *Journal of Spacecraft and Rockets*, Vol. 13, No. 3, pp 163-167, 1976.

[3] Vondra R. J., Thomassen K. I., "Performance Improvements in Solid Fuel Microthrusters", *Journal of Spacecraft*, Vol. 9, No. 10, September 1972.

[4] Guman W.J. and Nathanson, D.M., "Pulsed Plasma Microthruster Propulsion System for Synchronous Orbit Satellite," *Journal of Spacecraft*, vol. 7, No. 4, pp.409-415, 1970.

[5] Schonherr T et al, "Influence of Electrode Shape on Performances of Pulsed Magnetoplasmadynamic Thruster SIMPL-LEX", *Journal of Propulsion and Power*, Vol. 25, No. 2, 2009.

[6] Schonherr T et al, "Thrust efficiency optimization of the pulsed plasma thruster SIMP-LEX", *Acta Astronautica*, Vol. 67, pp 440-448, 2010.

[7] Tahara H. et al, "Flowfield Calculation of Electrothermal Pulsed Plasma Thrusters for the PROITERES Satellites", IEPC-2011-037, *32nd International Electric Propulsion Conference (Wiesbaden, Germany)*

[8] Edamitsu T. and Tahara H., "Performance Measurement and Flowfield Calculation of an Electrothermal Pulsed Plasma Thruster With A Propellant Feeding Mechanism", IEPC-2005-105, *29th International Electric Propulsion Conference*

[9] Keidar M., Boyd I. D., Antonsen E. L., Burton R. L., and Spanjers G. G., "Optimization Issues for a Micropulsed Plasma Thruster", *Journal of Propulsion and Power*, Vol. 22, No. 1, 2006.

[10] Keidar M. et al, "Analyses of Teflon Surface Charring and Near Field Plume of a Micro-Pulsed Plasma Thruster", IEPC-2001-155, *27th International Electric Propulsion Conference*

[11] Raizer Y.P., *Gas Discharge Physics*, 1991, Springer-Verlag, Berlin.

[12] Lifshitz E.M., Pitaevskii L.P. *Physical Kinetics: Volume 10 (Landau and Lifshitz: Course of Theoretical Physics)*, 1981, Pergamon Press, Oxford

[13] Smirnov B.M., *Plasma Processes and Plasma Kinetics*, 2007, WILEY-VCH Verlag. Weinheim

[14] Keider, M., Boyd, I. D., and Beilis, I. I., "Model of an Electrothermal Pulsed Plasma Thruster," *Journal of Propulsion and Power*, Vol. 19, No. 3, 2003, pp. 424-430.

[15] Ruchti C., Niemeyer L., "Ablation Controlled Arcs", *IEEE Trans. Plasma Sci.*, Vol. PS-14, No. 4, pp.423-434, 1986.

[16] Christen T., "A maximum entropy production model for Teflon ablation by arc radiation" *J Phys D: Appl. Phys*, Vol.40, pp. 5719-5722, 2007.

[17] Seeger M., Tepper J., Christen T., Abrahamson J., "Experimental study on PTFE ablation in high voltage circuit-breakers", *J Phys D: Appl. Phys*, Vol.39, pp. 5016–5024, 2006.